Dispersal sweepstakes: biotic interchange propelled air breathing fishes across the globe

Short title: Phylogenomics of synbranchiform fishes

Authors:

Richard C. Harrington. Dept. of Ecology and Evolutionary Biology, Yale University, USA.

Matthew Kolmann. Dept. of Biology, University of Louisville, USA.

Julia J. Day. Dept. of Genetics, Evolution and Environment, University College London, UK.

Brant C. Faircloth, Dept. of Biological Sciences and Museum of Natural Science, Louisiana State University, USA

Matt Friedman, Museum of Paleontology and Dept. of Earth and Environmental Sciences, University of Michigan, USA.

Thomas J. Near, Dept. of Ecology and Evolutionary Biology and Peabody Museum, Yale University, USA.

Corresponding Author: Richard C. Harrington, South Carolina Department of Natural Resources, Marine Resources Division, 331 Fort Johnson Road, Charleston, South Carolina, 29412. HarringtonR@dnr.sc.gov.

ABSTRACT

Aim: Biotic interchanges between Africa, India, and Eurasia are central to explaining the present-day distribution and diversity of freshwater organisms across these landmasses. Synbranchiformes is a diverse and species rich clade of freshwater acanthomorph fishes found on all southern continents except Antarctica, and include eel- and perch-like, air-breathing and non-air-breathing fishes. Lacking a comprehensive and resolved phylogeny of the entire clade,

contemporary interpretations of synbranchiform biogeography invoke scenarios as disparate as Gondwanan vicariance and pan-global rafting to explain their modern-day distribution. Here, we study their biogeographic history of continental dispersal events and test whether these are associated with increases in lineage diversification.

Location: Asia, India, Africa freshwater habitats

Taxon: Synbranchiformes (gouramis, snakeheads, swamp eels, and relatives)

Methods: We used nearly 1,000 ultra-conserved elements (UCEs) and Sanger-sequenced genes to infer a phylogeny with representatives of all major synbranchiform lineages and nearly two-thirds of its known species diversity. Incorporating fossil calibrations, we inferred a time-calibrated phylogeny to which we apply Bayesian methods of ancestral area reconstruction and test for diversification rate shifts.

Results: Analyses of UCE data provide a resolved phylogeny for major synbranchiform lineages. Divergence times support a most recent common ancestor of the entire clade approximately 79.2 million years ago. We infer significant increases in lineage diversification in both the spiny eels (Mastacembelidae) and the genus *Betta* (Osphronmeidae).

Main Conclusions: Our results reject the hypothesis of Gondwanan vicariance explaining synbranchiform biogeography. Instead, our analyses reconstruct a southeast Asian origin of the entire clade and independent dispersal events to other continents by snakeheads, anabantids, and spiny eels, with no signal of elevated lineage diversification occurring after these invasions. Higher lineage diversification rates in spiny eels pre-date their arrival to Africa, while the high diversification rates observed in *Betta* were initiated prior to the flooding of insular Sundaland in southeast Asia.

Keywords: *Betta*, labyrinth organ, pre-Pleistocene, Biogeography, India, Sundaland

INTRODUCTION

Freshwater fishes have served as models for studying biogeographic processes at nearly every spatial scale due to their limited ability to disperse outside of freshwater habitats and often narrow ecological niches within these environments (Olden et al., 2010). Pairing the best available understanding of lineage relationship and their divergence times with geographic distributions has been influential in formulating hypotheses about the history and mechanisms driving fish faunal diversification. This approach is essential when considering lineages with widespread distributions across multiple continents (Capobianco & Friedman, 2019). Phylogeny represents a necessary component of historical biogeography as the framework for analyzing geographic distributions. The proliferation of molecular data for phylogenetic analysis has drastically altered the resolution of the fish Tree of Life and provided a wealth of time-calibrated phylogenies that can be used to reexamine longstanding assumptions about freshwater fish biogeography (Dornburg & Near, 2021). For example, time-calibrated molecular phylogenies have both corroborated and contradicted long held assumptions of Gondwanan continental vicariance of lungfishes (Brownstein et al., 2023) and cichlids (Friedman et al., 2013; Matschiner et al., 2020) respectively. The rapidly emerging molecular phylogenetic perspective of fish systematics highlights the need to continuously reassess biogeographical hypotheses of the origins of freshwater fish diversity.

Synbranchiformes is a clade whose composition has recently changed as a result of molecular phylogenetic analyses. It is the only major clade (i.e., taxonomic Order) of Acanthomorpha that is composed entirely of primary freshwater fishes and also has a nearly

global distribution that can provide insight on continental patterns of biogeography (Betancur-R et al., 2013; Ghezelayagh et al., 2022; Near et al., 2013). The major lineages of Synbranchiformes are phenotypically diverse and include fishes that are perch-like (e.g., gouramis and snakeheads, Osphronemidae and Channidae respectively, Figure 1B,D), eel-like (swamp eels and spiny eels, Synbranchidae and Mastacembelidae, respectively, Figure 1F,G), and armored (*Indostomus*; Figure 1H). Synbranchiform species diversity is concentrated in Southeast Asia and India which contain over 60% of total species richness, with a secondary concentration of diversity in Sub-Saharan Africa. Some lineages are regionally endemic, such as *Betta* (85 species) and *Parosphromenus* (20 species), both of which are distributed in the Sundaland region of tropical Southeast Asia. Anabantidae, Channidae, Mastacembelidae, and Synbranchidae are widely distributed in both Africa and Asia. Two lineages of Synbranchidae, *Synbranchus* and *Ophisternon*, are distributed in Central and South America (Figure 1). The geological history of the tropical regions of Asia and Africa, particularly the tectonic rearrangements of India and Africa relative to Asia, highlight the geographic distribution of Synbranchiformes as an interesting target for historical biogeography (Capobianco & Friedman, 2019).

Past considerations of synbranchiform biogeography involve three hypotheses: (1) “Out of India” (Capobianco & Friedman, 2019; Chatterjee et al., 2013), (2) origination and dispersal from Southeast Asia (Darlington, 1957; Kosswig, 1955; Steinitz, 1954) and (3) Gondwanan vicariance (Britz, 1997; Britz et al., 2020). The latter hypothesis posits vicariance resulting from the fragmentation of Gondwana, while the former two propose dispersal from Asia to Africa and beyond from their respective centers of origin– either insular India as a 'biotic ferry' or from Southeast Asia (Capobianco & Friedman, 2019; Liem, 1963). All three hypotheses make explicit

predictions about timing and historical distributions that can be evaluated from temporal estimates and biogeographic reconstructions (Table 1). Although these predictions are explicit, several synbranchiform traits suggest they may have elevated dispersal ability relative to other freshwater fishes, complicating the interpretation of these scenarios. These traits include their ability to tolerate hypoxic aquatic environments using a variety of adaptations for breathing air from the water's surface via air-breathing organs (Tate et al., 2017), and the ability of some species to traverse over land (Das, 1928; Duan et al., 2018; G. M. Hughes & Munshi, 1979; Ishimatsu & Itazawa, 1981).

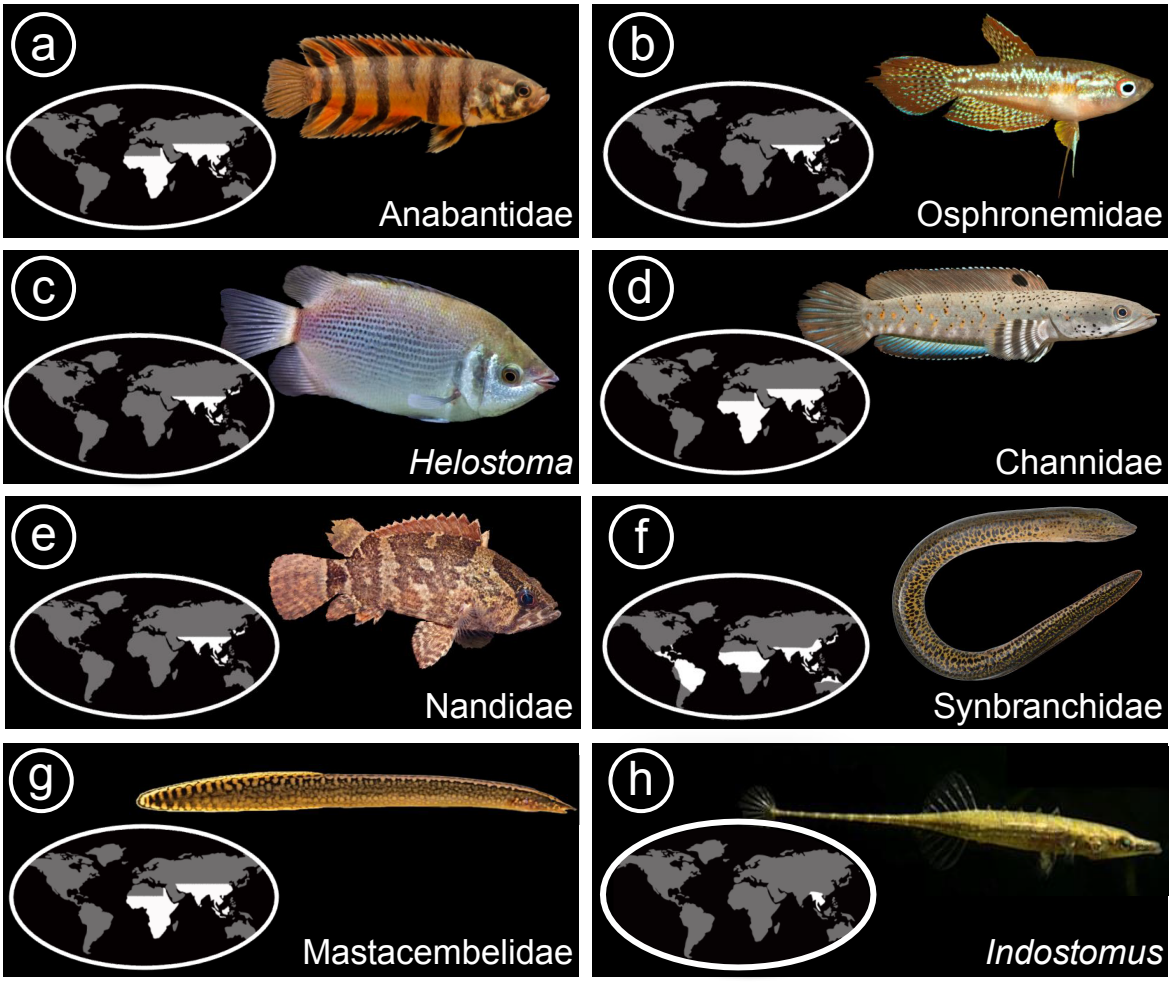

Figure 1 - Global range maps of major synbranchiform lineages. (A) climbing perches (Anabantidae), (B) gouramis, bettas, and pike gouramis (Osphronemidae), (C) Kissing Gourami

(*Helastoma*), (D) snakeheads (Channidae), Asian leaffishes (Nandidae), (F) swamp eels (Synbranchidae), (G) spiny eels (Mastacembelidae), (H) and armored sticklebacks (*Indostomus*). Not pictured: earthworm eels (Chaudhuriidae). [double column]

The ecological opportunities that result from a lineage moving to a previously unoccupied area are hypothesized to increase lineage diversification (Simpson, 1953; Stroud & Losos, 2016). However, studies that quantify diversification rates around geographic colonization events in island and continental settings suggest that this process needs to be studied on a case-by-case basis (Burbrink & Pyron, 2010; Harmon et al., 2008; Tran, 2014). The distribution of synbranchiform lineages across multiple continents poses historical biogeographical scenarios that may factor into variable lineage diversification dynamics, and understanding the role of biogeography in synbranchiform evolution is a critical step in assessing if dispersal to new areas was an important catalyst of their diversification.

Several studies have investigated the biogeographic history of individual clades within synbranchiforms – anabantids, channids, and mastacembelids in particular – but all make contrasting inferences regarding the origin and diversification of these lineages across the Paleotropics (Britz et al., 2020; Lavoué, 2020; Wu et al., 2019). Reconstructing the evolutionary history of these lineages requires a perspective on the biogeography of Synbranchiformes as a whole, which could refine the biological consequences of important Earth history events including the collision of insular India with Asia, the uplift of the Tibetan plateau, and the inundation of Sundaland (Britz et al., 2020; Lavoué, 2020; Wu et al., 2019). Additionally, the propensity for dispersal and invasion exhibited by members of some groups, like channids and synbranchids, raises questions about how shifting geographic distributions might have influenced the macroevolutionary history of certain lineages.

To address these questions, we generated a phylogeny using DNA sequence data collected from nearly 1,000 ultraconserved elements (UCEs) that includes representatives from all major lineages of Synbranchiformes. We expanded the taxonomic coverage offered in the UCE-inferred phylogeny by combining our UCE dataset with data obtained from Genbank, resulting in a phylogeny of Synbranchiformes that includes 64% of the species in the clade. We used this expanded tree to estimate divergence times among lineages to: (1) reconstruct the biogeographic history of Synbranchiformes in relation to Earth history events and (2) explore whether any inferred regional invasions are coincident with changes to lineage diversification in Synbranchiformes.

METHODS

UCE data generation and pipeline

We collected UCE sequence data from 124 species of Synbranchiformes and combined these with existing data from 35 acanthomorph outgroups collected as part of previous studies (Friedman et al., 2019; Harrington et al., 2016). Museum voucher information and NCBI SRA accession numbers are listed in Table S1. We used protocols described in Alfaro (2018) for DNA extraction, library preparation and enrichment, sequencing, and processing of sequence data. Detailed descriptions can be found in the Supporting Information.

Phylogenetic Inference

The UCE matrix included 159 species and phylogenetic analyses utilized UCE alignments that included at least 120 taxa for each locus (75% taxonomically complete). We determined the optimal partitioning strategy for the UCE-only dataset using PartionFinder v 2.1.1 (Lanfear et al., 2017), under a relaxed clustering search algorithm (Lanfear et al., 2014)

with UCE loci treated as individual units for partitioning, and we used the Bayesian Information Criterion for model comparison and selection. We inferred a maximum likelihood tree using IQ-Tree v 1.6.12. The tree search was conducted with IQTree's ultrafast bootstrap approximation, optimized by nearest neighbor interchange (Hoang et al., 2018), with 1000 bootstrap replicates and a GTR+G model of molecular evolution.

We inferred a coalescent-based species tree from UCE gene trees using ASTRAL v 4.11.1 (Zhang et al., 2018). Individual gene trees were inferred for each UCE locus that was at least 75% taxonomically complete using IQ-Tree, employing IQ-Tree's implementation of ModelFinder, followed by an SH-like approximate likelihood ratio test tree search, with 1,000 bootstrap replicates. The individual UCE locus gene trees were used as input for the ASTRAL coalescent species tree inference.

We estimated gene- and site-concordance factors in IQ-TREE 2 to assess topological congruence across our dataset by comparing the topology of individual gene trees to the topology inferred through concatenated analysis,. The concordance analysis in IQ-TREE 2 estimated the proportion of decisive individual UCE loci's gene trees (gCF) consistent with each branch in the phylogeny inferred through concatenation of the 75% complete UCE-only matrix. Site concordance factors (sCF) were calculated for each branch in the phylogeny based on one hundred randomly subsampled quartets from the 75% complete UCE-only concatenated alignment.

While the major lineages of Synbranchiformes were sampled in the UCE-only dataset, taxon sampling at the species level was not adequate to test biogeographic hypotheses. Therefore, we created a second, composite matrix that included taxa and data from the UCE-only data matrix as well as DNA sequences from four genes (*cytb*, *COI*, *rag1,* and *snx33*) obtained

from Genbank, which added 138 species of Synbranchiformes that were not represented in the UCE-only data matrix. Genbank accession numbers for these additional sequences are provided in Table S1. We were able to combine these two data sets because our target enriched UCE libraries usually contain DNA sequences from mitochondrial genomes. We used Phyluce to extract sequences of mitochondrial genes *cytb* and *COI* from sequenced libraries, and we aligned these sequences with those obtained from Genbank using MAFFT v 7.475. To investigate differences among topologies inferred from different loci, we inferred individual gene trees for *cytb*, *COI*, *rag1*, and *snx33* with IQ-Tree, using IQ-Tree's ModelFinder command to obtain the optimal partitioning strategy within each gene by codon position, and then used an SH-like approximate likelihood ratio test tree search with 1000 bootstrap replicates.

We also used Phyluce to build a concatenated data set containing the UCE data, the mitochondrial gene sequences extracted from sequenced libraries, and the mitochondrial and nuclear data downloaded from Genbank (UCE-composite matrix). To reduce the amount of missing data in downstream phylogenetic analyses among the taxa from the UCE-only matrix, we included UCE loci that were at least 95% taxonomically complete. For analysis of the UCE-composite matrix, we attempted several partitioning strategies, including: non-partitioned; full partitioning of the UCE portion of the matrix, with *cytb*, *COI*, *rag1* and *snx33* each given their own partition; and an analysis where *cytb*, *COI*, *rag1* and *snx33* were partitioned by codon position. While all partitioning strategies resulted in identical phylogenetic inferences with regards to the UCE-only dataset, the resolution of two species represented by only *COI* or *cytb* was variable in the trees resulting from analyses of different partitioning schemes of the Sanger sequenced loci (e.g., the position of *Mastacembelus alboguttatus* and the monophyly of *Belontia*).

196

197 *Divergence Time Estimation*

198 We used a node-based calibration strategy to estimate divergence times among species
199 using BEAST v 2.5.2 (Bouckaert et al., 2019), with a relaxed lognormal clock model and birth-
200 death tree branching model. A detailed justification and description of the 22 fossil-based
201 calibration priors is presented in the Supporting Information. We time-calibrated both the UCE-
202 only and UCE-composite tree topologies from IQ-Tree analysis of concatenated matrices. Due to
203 computational limitations, we followed previous acanthomorph phylogenomic studies and
204 conducted all divergence time analyses using subsets of randomly selected UCE loci (Friedman
205 et al., 2019). For both UCE-only data set, we selected three subsets of 30 UCE loci, and for the
206 UCE-composite data set, we selected three subsets of 30 UCE loci in addition to *COI, cytb,* and
207 *Rag1.* Optimal partitioning schemes were estimated with PartitionFinder 2.1.1, under a rcluster
208 heuristic search and GTR+Gamma model of evolution. UCE loci were treated as individual units
209 for partitioning, and codon positions treated separately for the three protein-coding loci. After
210 partitioning, we performed five replicates of each analysis for 250 million generations, with a
211 burn-in of 200 million generations discarded from each BEAST analysis, resampling every
212 50,000 trees, and combining and annotating summary maximum clade credibility (MCC) trees in
213 LogCombiner and TreeAnnotator, respectively. Log files from each replicate analysis were
214 viewed in Tracer 1.7 (Rambaut et al., 2018) to confirm convergence of parameter estimates
215 among runs and assess ESS values. Comparative analyses of biogeography and lineage
216 diversification were performed on the MCC time-tree inferred on the UCE-composite matrix.

217

218 *Model-Based Reconstruction of Synbranchiform Historical Biogeography*

We assigned current native geographic ranges to species based on distributional descriptions in FishBase species accounts (Froese & Pauly, 2022) using the following categories: Africa, India, Palearctic, Sundaland, Australia, and the Neotropics. We estimated ancestral ranges using the BioGeoBears v. 1.1.1 package (Dupin et al., 2017; Matzke, 2018) in the R v4.0.2 software platform. We applied several models of range evolution, including dispersal-extinction-cladogenesis (DEC) and BioGeoBears' likelihood interpretation of dispersal-vicariance (DIVA-Like) and BayArea (BayArea-Like) models (Landis et al., 2013). We also performed ancestral range reconstructions using these models with an additional 'jump' dispersal parameter that allows for founder events at cladogenesis, i.e., dispersal-mediated cladogenesis. To better reflect the likelihood of dispersal between continents that transition from being separated to connected at different times through the history of synbranchiform evolution, we implemented a time-stratified analysis in which a dispersal probability matrix was applied to three different time periods that reflect connectedness among land masses over the past tens of millions of years (Aitchison et al., 2007; Ali & Aitchison, 2008; Chatterjee et al., 2017): prior to 55 Ma, before a direct land connection between India and Asia; 55-30 Ma, corresponding to the duration of the India-Asia collision; and 30 Ma to the present, representing an essentially modern configuration between Asia and the Indian Subcontinent. See Table S2 for a detailed dispersal matrix for each time partition. We selected the model best fitting the data using the Akaike Information Criterion (AIC).

Diversification analyses

We tested for shifts in lineage diversification rates in the evolutionary history of Synbranchiformes using BAMM v2.5.0 (Rabosky, 2014). This method uses a reversible-jump

Markov chain Monte Carlo (rjMCMC) to quantify evolutionary rate heterogeneity. We inferred diversification rates using the 'speciation-extinction' setting in BAMM, which detects rate shifts along branches according to a Poisson process. We ran MCMCs with four chains for 50 million generations each, sampling every 5,000 generations. We accounted for incomplete taxon sampling by incorporating a sampling probability that considers the known global proportion of missing species from our phylogeny (including outgroups = 0.09), as well as genus-specific proportions of missing species. All priors were set as recommended by the 'setBAMMpriors' function in the *BAMMtools* package v2.1.7 (Rabosky et al., 2014), and we ran BAMM multiple times with the 'expectedNumberOfShifts' parameter set to 0.1, 1, 5, and 10. We used the *coda* package (Plummer et al., 2006) to evaluate convergence and examined the log-likelihoods of the MCMC output file to ensure that effective sample sizes (ESS) exceeded 200, after discarding 10% of posterior samples as burn-in. We determined the maximum a posteriori probability (MAP) shift configuration (the distinct shift configuration with the highest posterior probability) using the 'getBestShiftConfiguration' function and retained these results for further analyses.

BAMM has been criticized with respect to how non-global sampling fractions may shift the position of regime changes, or obscure where these regime shifts actually occur (Moore et al., 2016), but see an alternative perspective in Rabosky et al. (2017). Therefore, we also performed diversification analyses with MiSSE, a State-dependent Speciation and Extinction (SSE) model in the R package hisse (Beaulieu & O'Meara, 2016). MiSSE provides a framework for inferring diversification, speciation, and extinction rate differences using hidden states alone, which can account for rate heterogeneity among clades. We ran MiSSE using 26 possible hidden rate configurations, varying net turnover and holding extinction fraction consistent across all models (eps = 1). We chose the model with the lowest AICc as the preferred scenario; however, MiSSE

allows for model averaging among models with similar AIC scores, and this was used to account for subtle differences in the best-supported models.

RESULTS & DISCUSSION

Summary of sequence data

A summary of data matrices used to perform phylogenetic and divergence time analyses is provided in Table S3. Our sequencing efforts produced a 75% complete matrix composed of 998 UCE loci, with a mean length of 614 bp and 276 parsimony informative sites per locus. The total length of the concatenated 75% complete matrix was 612,737 bp. The 95% complete matrix included 674 loci, with a mean of 656 bp length and 298 parsimony informative sites per locus, and a total concatenated length of 441,224 base pairs. The protein-coding mitochondrial loci *COI* and *cytb* alignments are 688 bp and 1,144 bp, respectively, and the nuclear *rag1* and *snx33* alignments are 1,497 bp and 739 bp, respectively. The phylogeny inferred from the UCE-composite dataset is shown in Figures 2-3. Figures in the Supporting Information include the tree inferred from the UCE-only dataset (Figure S1), the phylogeny inferred from the UCE-composite dataset that includes all sampled species (Figure S2), the ASTRAL coalescent-based tree (Figure S3), and the gene trees inferred from *COI*, *cytb*, *rag1*, and *snx3* (Figures S4 - S7, respectively).

Phylogeny of Synbranchiformes

Prior to the use of molecular data to investigate the phylogenetics of acanthomorph fishes, studies of morphology suggested a close relationship among the lineages that comprise Anabantoidei and Synbranchoidei (Berg, 1940; Lauder & Liem, 1983; D. E. Rosen & Patterson,

1990). Molecular phylogenetic analyses consistently resolve Synbranchiformes as monophyletic (Betancur-R et al., 2013; Chen et al., 2003; L. C. Hughes et al., 2018; B. Li et al., 2009; Near et al., 2013; Wainwright et al., 2012). The phylogenetic analyses of the UCE-only and UCE-composite datasets support the monophyly of Synbranchiformes and two major subclades: the Synbranchoidei containing *Indostomus*, Synbranchidae, Chaudhuriidae, and Mastacembelidae and Anabantoidei containing Nandidae, Channidae, Anabantidae, *Helostoma temminckii*, and Osphronemidae (Figure 2, 3 and S1). We delimit Nandidae as containing species of *Nandus*, *Badis*, *Dario*, and *Pristolepis* (Figure 2). Alternatively, these four genera are classified into three taxonomic families, two of which contain a single genus (Betancur-R et al., 2017; Nelson et al., 2016:394-395). Our delimitation of Nandidae is reflected in previous classifications (Nelson, 2006:381-383) and is consistently resolved in molecular phylogenetic analyses and supported with morphological apomorphies (Collins et al., 2015; Ghezelayagh et al., 2022; Near et al., 2013). The relationships among major subclades and species in the phylogenies inferred from UCE-only and UCE-composite datasets are broadly congruent (Figures 2, 3, S1, S2). The UCE-based molecular phylogenies have high node support values in both concatenated and coalescent-based analyses indicating that they are characterized by high levels of agreement among individual UCE gene trees (Figures S1, S3).

Within the Synbranchoidei, the phylogenies inferred using the UCE-only and UCE-composite matrices resolve two clades, one containing *Indostomus* and Synbranchidae and the other with Chaudhuriidae and Mastacembelidae (Figure 2, S1, S2). While studies of morphology suggested a relationship among Mastacembelidae, Chaudhuriidae, and Synbranchidae (Gosline, 1983; McAllister, 1968), ours is the first molecular phylogenetic study to resolve Chaudhuriidae and Mastacembelidae as sister taxa. Several morphological traits have been hypothesized to

represent synapomorphies that support the resolution of *Sinobdella* in Mastacembelidae (Britz, 1996; Kottelat & Lim, 1994), which is supported in the UCE-composite molecular phylogeny (Figure 2, S2). Our results are congruent with all previous molecular phylogenetic studies of Synbranchoidei, although these studies did not include either *Indostomus* or Chaudhuriidae (Betancur-R et al., 2013; L. C. Hughes et al., 2018; Near et al., 2013). In contrast to conclusions based on morphology (D.E. Rosen & Greenwood, 1976), the UCE phylogeny resolves the synbranchid lineage *Ophisternon* as paraphyletic relative to a clade containing two Neotropical species, *Synbranchus marmoratus* and *O. aenigmaticum* (Figure 2, S2).

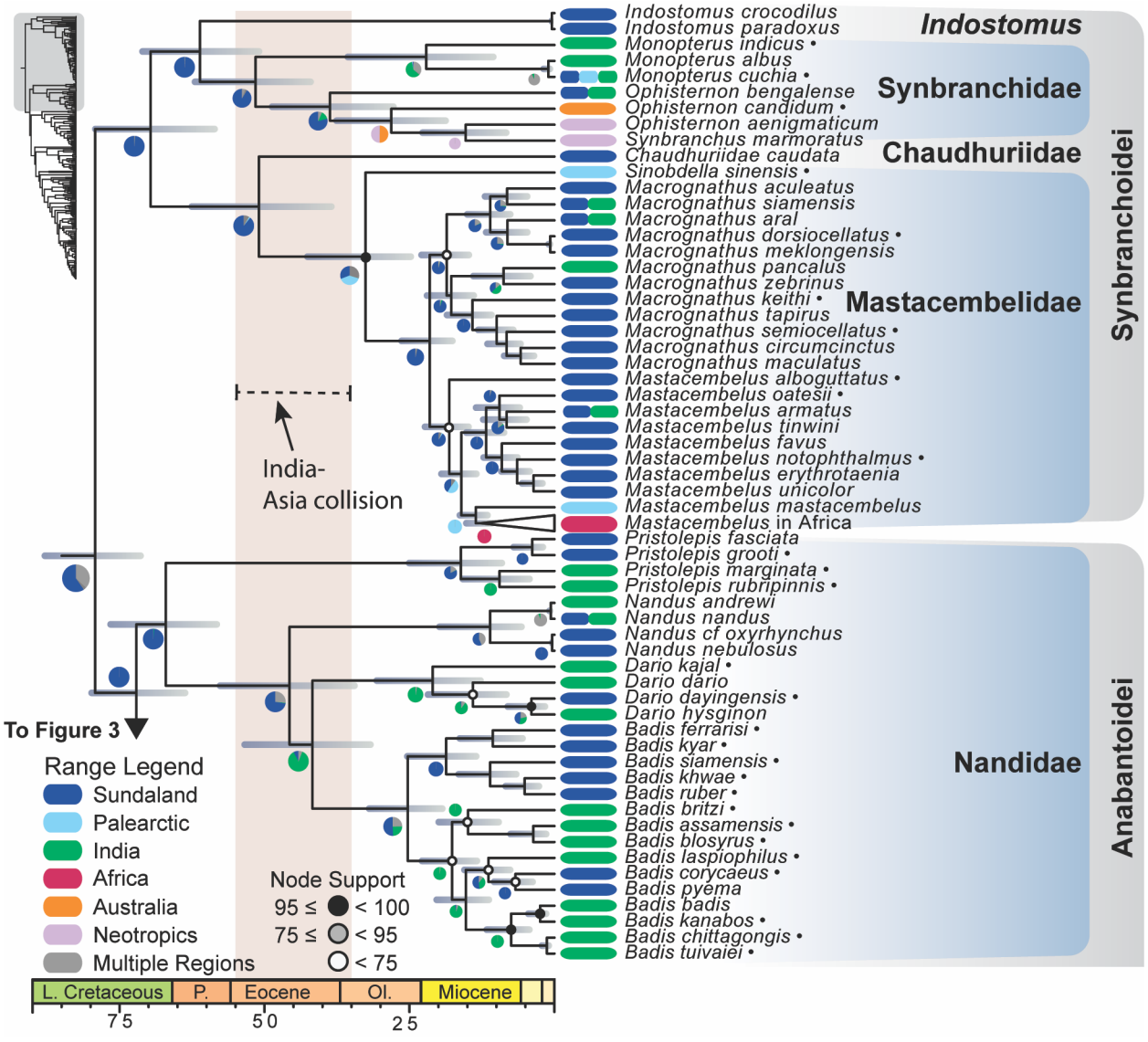

Figure 2 - Time-calibrated phylogeny and biogeographic history of Synbranchiformes based on BEAST analysis of UCE loci combined with *cytb*, COI, and *rag1*. Horizontal bars indicate 95% HPD of age estimates for each node. Ultrafast bootstrap support (UFBoot) values are represented as discs on each node. Black discs indicate UFBoot of between 95 and lower than 100, gray indicating 75 to 95, and white indicating UFBoot values lower than 75. Nodes without a disc indicate UFBoot support of 100. Geographic distributions of extant species are coded to the right of each species name. Biogeographical reconstructions of ancestral ranges inferred analysis in BioGeoBears under a DEC+J model are shown in pie charts adjacent to each node. Phylogeny continues on Figure 3. [double column]

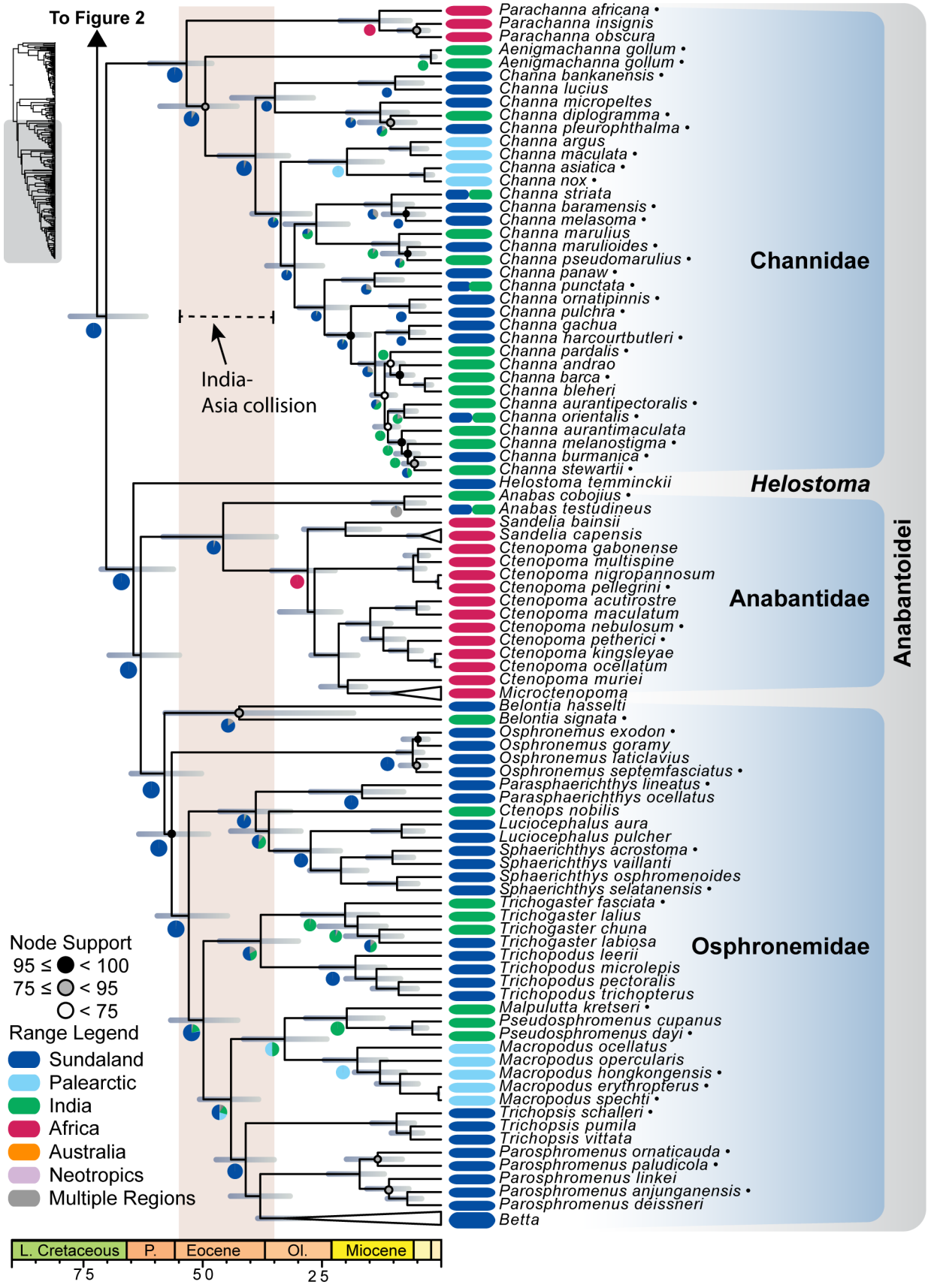
To Figure 2
India-
Asia collision
Parachanna africana •
Parachanna insignis
Parachanna obscura
Aenigmachanna gollum •
Aenigmachanna gollum •
Channa bankanensis •
Channa lucius
Channa micropeltes
Channa diplogramma •
Channa pleurophthalma •
Channa argus
Channa maculata •
Channa asiatica •
Channa nox •
Channa striata
Channa baramensis •
Channa melasoma •
Channa marulius
Channa marulioides •
Channa pseudomarulius •
Channa panaw •
Channa punctata •
Channa ornatipinnis •
Channa pulchra •
Channa gachua
Channa harcourtbutleri •
Channa pardalis •
Channa andrao
Channa barca •
Channa bleheri
Channa aurantipectoralis •
Channa orientalis •
Channa aurantimaculata
Channa melanostigma •
Channa burmanica •
Channa stewartii •
Helostoma temminckii
Anabas cobojius •
Anabas testudineus
Sandelia bainsii
Sandelia capensis
Ctenopoma gabonense
Ctenopoma multispine
Ctenopoma nigropannosum
Ctenopoma pellegrini •
Ctenopoma acutirostre
Ctenopoma maculatum
Ctenopoma nebulosum •
Ctenopoma petherici •
Ctenopoma kingsleyae
Ctenopoma ocellatum
Ctenopoma muriei
Microctenopoma
Belontia hasselti
Belontia signata •
Osphronemus exodon •
Osphronemus goramy
Osphronemus laticlavius
Osphronemus septemfasciatus •
Parasphaerichthys lineatus •
Parasphaerichthys ocellatus
Ctenops nobilis
Luciocephalus aura
Luciocephalus pulcher
Sphaerichthys acrostoma •
Sphaerichthys vaillanti
Sphaerichthys osphromenoides
Sphaerichthys selatanensis •
Trichogaster fasciata •
Trichogaster lalius
Trichogaster chuna
Trichogaster labiosa
Trichopodus leerii
Trichopodus microlepis
Trichopodus pectoralis
Trichopodus trichopterus
Malpulutta kretseri •
Pseudosphromenus cupanus
Pseudosphromenus dayi •
Macropodus ocellatus
Macropodus opercularis
Macropodus hongkongensis •
Macropodus erythropterus •
Macropodus spechti •
Trichopsis schalleri •
Trichopsis pumila
Trichopsis vittata
Parosphromenus ornaticauda •
Parosphromenus paludicola •
Parosphromenus linkei
Parosphromenus anjunganensis •
Parosphromenus deissneri
Betta
Channidae
Helostoma
Anabantidae
Osphronemidae
Anabantoidei
Node Support
95 ≤ ● < 100
75 ≤ ● < 95
○ < 75
Range Legend
Sundaland
Palearctic
India
Africa
Australia
Neotropics
Multiple Regions
L. Cretaceous
P.
Eocene
Ol.
Miocene
75
50
25

Figure 3 - Time-calibrated phylogeny (continued from Figure 2) and biogeographic history of Synbranchiformes based on BEAST analysis of UCE loci combined with *cytb*, COI, and *rag1*. Horizontal bars indicate 95% HPD of age estimates for each node. Ultrafast bootstrap support (UFBoot) values are represented as discs on each node. Black discs indicate UFBoot of between 95 and lower than 100, gray indicating 75 to 95, and white indicating UFBoot values lower than 75. Nodes without a disc indicate UFBoot support of 100. Geographic distributions of extant species are coded to the right of each species name. Biogeographical reconstructions of ancestral ranges inferred analysis in BioGeoBears under a DEC+J model are shown in pie charts adjacent to each node. [double column]

Phylogenetic analyses of the UCE-only and UCE-composite matrices resolve *Macrognathus* and *Mastacembelus* as reciprocally monophyletic sister lineages (Figure 2, S1). Previous molecular phylogenetic studies of relationships within Mastacembelidae densely sampled African species but included a sparse sampling of Asian species as outgroups (Alter et al., 2015; Brown et al., 2010; Day et al., 2017). Where the species-level sampling overlaps, the relationships among major species groups and their composition inferred from the UCE-only and UCE-composite matrices are broadly congruent with the phylogenies inferred in Day et al. (2017).

The UCE-inferred phylogeny of Synbranchiformes (Figure 3) is congruent with previous morphological analyses in resolving a clade that contains lineages with the labyrinth-organ: *Helostoma*, Anabantidae, and Osphronemidae (Britz, 1994). Most incongruence among previous phylogenetic hypotheses is due to the variable resolution of Channidae as either the sister group of the labyrinth-organ clade (Britz et al., 2020; L. C. Hughes et al., 2018; Near et al., 2013;

Sanciangco et al., 2016; Springer & Johnson, 2004; Wu et al., 2019) or Nandidae (Betancur-R et al., 2013), and *Helostoma* as either the sister taxon of Anabantidae (Britz et al., 2020; Collins et al., 2015; L. C. Hughes et al., 2018), Osphronemidae (Betancur-R et al., 2013; Near et al., 2013; Rüber et al., 2006; Sanciangco et al., 2016), or a clade containing Anabantidae and Osphronemidae (Collins et al., 2015). The phylogenies resulting from analysis of all concatenated datasets resolve Channidae (which also has a labyrinth-like air-breathing organ) as the sister taxon of the labyrinth-organ clade, and *Helostoma* as the sister taxon of a clade comprising Anabantidae and Osphronemidae (Figure 3, S1).

Phylogenetic relationships among genera and among species groups within genera of Anabantoidei inferred from the UCE-only and UCE-composite matrices are mostly congruent with those found in previous analyses based on smaller numbers of loci (Adamson et al., 2010; Britz et al., 2020; X. Li et al., 2006; Rüber, Britz, Kullander, et al., 2004; Rüber, Britz, Tan, et al., 2004; Rüber et al., 2006; Rüber et al., 2020); however, there remain several differences worth noting. Within Anabantidae, the UCE phylogeny places *Sandelia* as the sister taxon to a clade containing *Ctenopoma* and *Microctenopoma*, where *Ctenopoma* is paraphyletic relative to *Microctenopoma* (Figure 2). The concatenated and coalescent-based UCE-inferred phylogenies resolve *Belontia* as the sister taxon to all lineages of Osphronemidae (Figure 3, S1), as opposed to *Belontia* and *Osphronemus* as sister taxa in phylogenies resulting from analyses of Sanger-sequenced mtDNA and nuclear genes (Rüber et al., 2006; Wu et al., 2019). Our study confidently (100% UF bootstrap support in concatenated analysis; local posterior probability support of 1.0 in ASTRAL analyses of UCE-only matrices) confirms pike gouramies (*Luciocephalus*) and *Sphaerichthys* are sister taxa (Figure 3), and nested within Osphronemidae (Britz et al., 1995; Rüber et al., 2006), in contrast to a taxonomic classification of *Luciocephalus*

in a monotypic subfamily or suborder (Berg, 1940; Lauder & Liem, 1981; Liem, 1965, 1967). The morphological characters that once misled analyses of the phylogenetic affinity of *Luciocephalus* (e.g., lack of parasphenoid teeth, reduced labyrinth organ) instead can be interpreted as losses or reductions following adaptations for piscivory.

Within Channidae, the phylogeny inferred from the UCE-composite dataset resolves *Parachanna* as the sister taxon of a clade comprising *Aenigmachanna* and *Channa* (Figure 3). In contrast, phylogenetic analysis of morphological data resolved *Aenigmachanna* as sister to a clade containing *Parachanna* and *Channa* (Britz et al., 2020). Molecular analyses presented by Britz et al. (2020) were conducted using a topological constraint to reflect the results of the phylogeny resulting from analysis of morphological characters. Phylogenetic analyses of the individual loci used in Britz et al. (2020) result in incongruent topologies regarding the placement of *Aenigmachanna* relative to other synbranchiform lineages (Figures S4-S7). Our molecular phylogenetic results do not support the placement of *Aenigmachanna* as the sister taxon of the clade comprising *Channa* and *Parachanna* (Figure 3). Even if *Aenigmachanna* represents the sister taxon of the clade containing *Channa* and *Parachanna,* it would still be most effectively classified in Channidae. The description of a monogeneric Aenigmachannidae provides no information on phylogeny and only accomplishes creating a group name that is redundant with *Aenigmachanna*. The limited number of loci sequenced for *Aenigmachanna* and the discordant or unresolved relationships inferred from these loci highlight the need for additional sequence data in order to resolve the relationships among *Aenigmachanna*, *Channa*, and *Parachanna*.

Timing and Geographic Context of Diversification

Divergence times estimated across replicate, fossil-calibrated relaxed clock analyses of UCE-only (Figure S8) and UCE-composite data matrices (Figures 2-3) converged on similar age estimates, with overlapping 95% highest posterior densities for ages at most nodes (Table 2). Here, we discuss specific dates obtained from an analysis of a sequence matrix that includes UCE loci, *COI*, *cytb*, and *rag1*. The BEAST analyses estimated the age of the most recent common ancestor (MRCA) of Synbranchiformes as 79.2 Ma [95% HPD: 70.8-88.5 Ma] during the Late Cretaceous. The ages of the MRCAs of Synbranchoidei and Anabantoidei are estimated as 69.7 Ma [95% HPD: 58.1-79.7 Ma] and 72.1 Ma [95% HPD: 63.2-80.4 Ma], respectively (Figures 2, 3, S2). The age estimates for lineages within both Synbranchoidei and Anabantoidei are similar to those resulting from other relaxed molecular clock analyses (Betancur-R et al., 2013; L. C. Hughes et al., 2018; Near et al., 2013), and these age estimates pre-date the hypothesized Eocene timing of initial contact between the Indian and Asian tectonic plates (Ali & Aitchison, 2008; Meng et al., 2012). Most major lineages of Synbranchiformes classified as taxonomic families began to diversify within the Paleocene and early Eocene (Figures 2, 3). Mastacembelidae, one of the most species-rich lineages of Synbranchiformes (93 species), has a relatively younger crown age of 32.6 Ma [95% HPD: 24.2-43.2 Ma].

The biogeographic setting and processes that shaped the present-day distribution of Synbranchiformes have previously been investigated with time-calibrated phylogenies to reconstruct ancestral geographic ranges (Lavoué, 2020; Wu et al., 2019). However, these were predominately focused on lower taxonomic levels, for example, the biogeographic history of the Channidae and the timing of the divergence between African and Asian lineages (Britz et al., 2020; Rüber et al., 2020). These studies estimated age estimates broadly congruent with ours, but lacked comprehensive inclusion of both Synbranchoidei and Anabantoidei that would permit

robust inferences regarding the geographic context of the most ancient divergences among the living lineages of Synbranchiformes.

AIC comparison of all tested models of geographic range evolution of Synbranchiformes favored the DEC + J model, and we discuss details of biogeographic history inferred under this model (Table 3). The DEC+J reconstruction of ancestral geographic ranges in Synbranchiformes strongly support a Southeast Asian origin for both Synbranchoidei and Anabantoidei (Figure 2). This model also inferred strong likelihood support for Southeast Asian origins of all major lineages of Synbranchiformes and indicated strong support for independent Asia-to-Africa dispersal events within Anabantidae, Channidae, and Mastacembelidae (Figures 2, 3). This conclusion contrasts with a previous historical biogeographic reconstruction that had equivocal likelihood support for the deepest nodes in Anabantoidei, and indicated higher likelihood of an Indian origin for Channidae (Wu et al., 2019). More precise constraints on the timing of these Asia-Africa dispersal events are limited by the long stems subtending the African lineages of Anabantidae and Channidae. The estimated crown ages for Anabantidae and Channidae are 45.7 and 53.3 Ma respectively (Figure 3), suggesting an earliest possible dispersal event in the early- to mid-Eocene. In contrast, the African clade of *Mastacembelus* has an estimated MRCA of 12.7 Ma, and the MRCA of this African clade and its sister lineage (*M. mastacembelus*, a species distributed in the Middle East) is 13.6 Ma (Figure 2), supporting a dispersal event between 16.9 to 10.2 Ma. The mean timing of this dispersal event is slightly younger than that estimated by Day et al. (2017), but within overlapping 95% HPD of the posterior age estimates.

Timeline for the origin of Synbranchiformes and implications for their biogeography

Our findings are inconsistent with the Gondwanan vicariance model in terms of timescale and reconstructed ancestral distribution. We infer the last common ancestor of Synbranchiformes

originated in Southeast Asia 79.2 [95% HPD: 70.8-88.5] million years ago. The older bound of this estimate substantially postdates the initial rifting of Gondwana that took place beginning in the early-mid Mesozoic, tens of millions of years earlier (Ali & Aitchison, 2008; Matthews et al., 2016). Indeed, Southeast Asia is the reconstructed ancestral distribution for every node in phylogeny of Synbranchiformes that is older than the Eocene (Figures 2, 3).

The remaining two hypotheses assume deep-time invasions from their points of origin, either India or Asia. The “Out of India" hypothesis proposes sporadic biotic connections between India and Africa during the northward tectonic movement of India toward Asia (Briggs, 2003; Chatterjee et al., 2013; Chatterjee & Scotese, 2010; Chatterjee et al., 2017), either in the form of land bridges (e.g., the Somali peninsula; Chatterjee & Scotese, 2010) or island-hopping (Briggs, 1989, 2003; Rage, 2003). However, geological evidence for the existence of these land bridges has been called into question (Aitchison et al., 2007; Ali & Aitchison, 2004, 2008). Our results suggest that no lineages of Synbranchiformes were present in freshwater habitats of the Indian subcontinent until the Eocene (Figures 2, 3), corresponding to the earliest unambiguous fossil channid remains from the middle Eocene of Pakistan (Murray & Thewissen, 2008). The Asian origin hypothesis assumes dispersal of anabantoids via sporadic land connections between Eurasia and Africa through what is now the Middle East (Darlington, 1957:101; Kosswig, 1955; Liem, 1963:61-65; Steinitz, 1954). Liem (1963:61-65) hypothesized an Eocene age for Asian-African faunal interchange, whereas Steinitz (1954) and Kosswig (1955) proposed exchanges during the Miocene and Pliocene, respectively. Our results support the 'Out of Asia' scenario, given the reconstructed ancestral ranges of all major synbranchiform lineages is Southeast Asia and that dispersal events to other continents occur only at the culmination of India's collision with Asia. While synbranchiforms likely did not evolve on insular India, these results suggest

that the uplift of the Tibetan plateau may have isolated some lineages (e.g., *Macropodus*, *Sinobdella*) while facilitating the spread of others (snakeheads, climbing perches (Wu et al. 2019)).

The historical biogeographic reconstructions infer three separate dispersals to Africa by lineages within Channidae, Anabantidae, and Mastacembelidae (Figures 2, 3). The African arrival of *Mastacembelus* is estimated to have occurred during the Miocene. The African lineage of Anabantidae dates at least to the Oligocene, sharing a common ancestor with the pan-Asian *Anabas* that dates to the Eocene (Figure 3). The MRCA of *Parachanna*, which represents the African lineage of Channidae, dates to the Miocene, but fossil evidence indicates dispersal to Africa no later than the early Oligocene (Murray, 2012). The dispersal to Africa from Asia occurred in at least two waves, with lineages of Channidae and Anabantidae arriving in the Paleogene, and mastacembelids arriving in the Neogene (Brown et al., 2010). A late Eocene invasion of Africa from Laurasia has also been noted for various mammal and reptile lineages based on fossil data (Gheerbrant & Rage, 2006). These invasions of Africa are reconstructed as unidirectional for each lineage (Figure 3), with no evidence of returns to Eurasia from Africa. The fossil record indicates that channids were found as far north and west as southern Germany during the middle Miocene, coincident with the presence of other African freshwater fishes in southern France (Gaudant, 2015; Gaudant & Reichenbacher, 1998). Interestingly, the arrival of channids in Europe and deeper within continental Asia coincides with the extirpation of their possible ecological analogs, bowfins (Amiidae), which are now only found in North America but are present in the central Asian and European fossil record until the Oligocene, with less definitive evidence from the Miocene (Grande & Bemis, 1998).

The most prodigious example of dispersal among living lineages of Synbranchiformes is the near global distribution of swamp eels (Synbranchidae), which occupy all southern continents except Antarctica (Figures 1, 2). Like all other lineages of Synbranchiformes, Synbranchidae and the MRCA of *Indostomus* and Synbranchidae are inferred to originate in Southeast Asia (Figure 2). The estimated age of Synbranchidae is 51.4 Ma [95% HPD: 41.5-62.6 Ma], reaffirming that their present-day distribution could not result from Gondwanan vicariance, as this date is well after the break-up of Gondwana. Although our findings show that South and Central American swamp eels are nested within wide-ranging taxa from Southeast Asia, New Guinea, and Northern Australia, the ability to interpret these biogeographical patterns is restricted by the absence of African synbranchids in our dataset. If swamp eels invaded Africa from Asia, as did lineages of Channidae, Anabantidae, this may have occurred during the Eocene. This scenario seems more probable given the age of synbranchid lineages, relative to more recent African arrivals like Mastacembelidae (Figure 2). The salinity tolerance, air-breathing ability, and fossoriality of swamp eels could make them capable rafters in large aquatic debris like tree trunks (Houle, 1998).

Lineage Diversification after Continental Invasion

Estimates of lineage diversification suggest that no shifts in diversification rates were concurrent with reconstructed continental invasions (Figures 2 - 4). Our analyses identified 9 out of 192 rate shift configurations which together comprise 51% of the cumulative probability. In all nine of these configurations, there is a rate shift at the MRCA of the clade containing *Mastacembelus* and *Macrognathus*, with another shift observed 8 of 9 times near the MRCA of *Betta* and sometimes including the MRCA of the clade containing *Betta*, *Parosphromenus* and

514 *Trichopsis* (Figure 4). According to the BAMM analyses, the clade containing *Mastacembelus*
515 and *Macrognathus* (0.167 species per million years) exhibits a rate of lineage diversification that
516 is nearly 2.5 times higher than other lineages of Synbranchoidei (0.068 species per million
517 years), while the clade containing *Betta*, *Parosphromenus* and *Trichopsis* (0.109 species per
518 million years) exhibits rates of lineage diversification that are more than 1.5 times higher than all
519 Osphronemidae (0.072 species per million years). No configurations were favored in BAMM
520 where there are zero rate shifts across the time-calibrated phylogeny of Synbranchiformes
521 (Figure 4). MiSSE results largely corroborated elevated diversification rates in the clade
522 containing *Mastacembelus* and *Macrognathus,* as well as the *Betta* clade. However, MiSSE did
523 not extend elevated rates of lineage diversification beyond *Betta*, to include *Parosphromenus* and
524 *Trichopsis*, as did BAMM analyses (Figure 4).
525 The significant shift towards higher diversification rates within spiny eels
526 (Mastacembelidae) occurs after the origin of the crown clade (MRCA of 32 Ma) and to the
527 exclusion of the monotypic *Sinobdella*. The clade containing *Macrognathus* and *Mastacemblus*,
528 which is distributed throughout Southeast Asia, India, and Africa, is characterized by a higher
529 rate of lineage diversification than all other synbranchiform clades, apart from *Betta* (Figure 4).
530 The estimated MRCA of the *Mastacembelus* + *Macrognathus* clade is 21.5 Ma [95% HPD: 17.0-
531 26.9 Ma], and this shift to a high diversification rate precedes both the radiation of
532 *Mastacembelus* in Lake Tanganyika and more generally the arrival of spiny eels in Africa
533 (Figure 2). Understanding modern spiny eel diversity requires a closer look at the origins of
534 mastacembelids in Asia and their continental movements from Southeast Asia into the Middle
535 East and then into Africa.

536 The estimated age of the MRCA of *Betta* is 33.2 Ma [95% HPD: 26.9-44.7 Ma] near the
537 Eocene-Oligocene boundary (ca. 34 Ma) and the estimated ages of the MRCAs of most of the
538 sampled species range between 10 and 1.5 My (Figure 3), suggesting their diversification was
539 not the result of Pleistocene events such as glacial cycles and sea level rise (Sholihah, Delrieu-
540 Trottin, Condamine, et al., 2021; Sholihah, Delrieu-Trottin, Sukmono, et al., 2021). Elevated
541 diversification in *Betta* might be a consequence of their limited capacity for dispersal,
542 preferences for acidic waters and peat swamps, and the presumably extreme habitat
543 fragmentation promoted by these narrow niche requirements. Sexual selection, arising from the
544 conspicuously complex mating systems in *Betta* as well as the closely related *Parosphromenus*
545 and *Trichopsis*, might also be responsible for catalyzing high speciation in these fishes (Rüber,
546 Britz, Tan, et al., 2004). Similar mating behaviors like mouth brooding or nesting, sexual
547 display, and male combat are thought to contribute to high net diversification identified in cichlid
548 fishes (Lande et al., 2001; Seehausen, 2000).

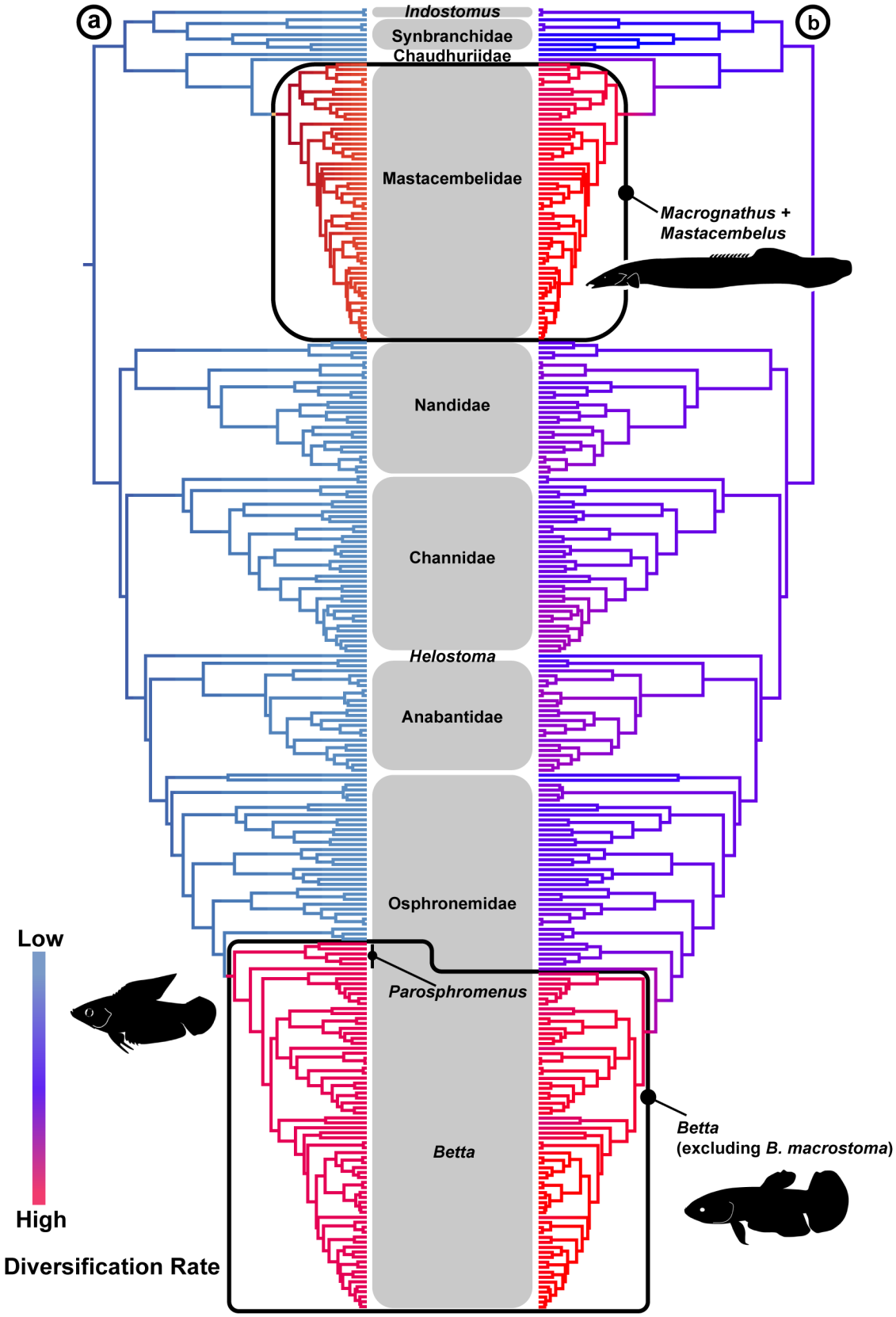
a
b
Indostomus
Synbranchidae
Chaudhuriidae
Mastacembelidae
Macrognathus +
Mastacembelus
Nandidae
Channidae
Helostoma
Anabantidae
Osphronemidae
Parosphromenus
Betta
Betta
(excluding B. macrostoma)
Low
High
Diversification Rate

549

Figure 4 - Lineage diversification analyses of Synbranchiformes. (A) BAMM, (B) MiSSE. Significant increases in diversification rates are noted in mastacembelids (sans *Sinobdella*) and the genus *Betta* (and sometimes its sister clade, *Parosphromenus*). Black boxes highlight clades of interest. [double column]

Extrinsic factors, like the repeated marine inundation and volatile geological history of Sundaland over the past 30 million years likely shaped the evolutionary history of *Betta* (Beamish et al., 2003; Hui & Ng, 2005a, 2005b). Different portions of Sundaland have been periodically covered by shallow marine waters several times during the last 30 million years, with the latest inundation occurring 14,000 years ago (Sholihah, Delrieu-Trottin, Condamine, et al., 2021). However, pre-Pleistocene geological activities are more likely to have shaped the modern diversity of *Betta* than recent island vicariance (Sholihah, Delrieu-Trottin, Sukmono, et al., 2021). This complicated geological history may explain why there is conspicuously higher diversity of *Betta* in areas of insular Sundaland that include Java, Borneo, and Sumatra than on mainland Sundaland or the Indo-Burma region (Kowasupat et al., 2012; Schindler & Schmidt, 2009).

Conclusions

The Synbranchiformes are a unique example of a major Order-level clade of acanthomorph teleosts that are entirely freshwater. The phylogenomic analyses we conducted resolve the relationships among the major lineages of Synbranchiformes. The phylogeny we inferred allows for a new delimitation where Badidae and Pristolepididae are treated as synonyms of Nandidae, and Aenigmachannidae is identified as a synonym of Channidae. Despite

competing hypotheses to explain the biogeographic history of Synbranchiformes, model-based reconstructions strongly support a southeastern Asian origin followed by a dispersal to India, the Middle East, Africa, and beyond. Moreover, these continental invasions, particularly into Africa, occurred in multiple waves that started during the Paleogene and Neogene. Analysis of lineage diversification detected no pattern indicative of continental invasions precipitating shifts in lineage diversification rates.

Data Availability

The UCE sequence data underlying this study are available from the NCBI Sequence Read Archive database, and can be accessed with BioProject numbers PRJNA892110, PRJNA341709, and PRJNA758064. All other data supporting this article are available in the Dryad Digital Repository, at https://dx.doi.org/10.5061/dryad.59zw3r2c0 . FOR REVIEWERS: The Dryad repository is not officially published, but can be accessed by reviewers with the following link: https://datadryad.org/stash/share/tvWDW_4cIu1FhwJESPycN-tWddVidwQqWOYDCkXamlk

Supporting Information

Data available from the Dryad Digital Repository: http://dx.doi.org/10.5061/dryad.[NNNN]

Funding

This work was supported by the Bingham Oceanographic Fund maintained by the Peabody Museum, Yale University to T.J.N.

Acknowledgements

The authors wish to thank our handling editor, Jonathan Waters, and two anonymous referees for providing constructive feedback that greatly improved the manuscript. The authors thank the

following for providing fish tissue and DNA samples: Cornell University Museum of Vertebrates, Prosanta Chakrabarty and the Louisiana State University Museum of Natural Science Ichthyology Collection, University of Florida, Brian Sidlauskas and Oregon State Ichthyology Collection, and the South African Institute of Aquatic Biology. We thank Oliver Lucanus and Mark Sabaj for providing images of live fishes used in Figures 1, and Samuel Borstein for assistance with diversification methods. No permits were required for this research.

References

Adamson, E. A. S., Hurwood, D. A., & Mather, P. B. (2010). A reappraisal of the evolution of Asian snakehead fishes (Pisces, Channidae) using molecular data from multiple genes and fossil calibration. *Molecular Phylogenetics and Evolution, 56*(2), 707-717. doi:https://doi.org/10.1016/j.ympev.2010.03.027

Aitchison, J. C., Ali, J. R., & Davis, A. M. (2007). When and where did India and Asia collide? *Journal of Geophysical Research-Solid Earth, 112*(B5). doi:Artn B05423 10.1029/2006jb004706

Alfaro, M. E., Faircloth, B. C., Harrington, R. C., Sorenson, L., Friedman, M., Thacker, C. E., . . . Near, T. J. (2018). Explosive diversification of marine fishes at the Cretaceous–Palaeogene boundary. *Nature Ecology & Evolution, 2*(4), 688-696. doi:10.1038/s41559-018-0494-6

Ali, J. R., & Aitchison, J. C. (2004). Problem of positioning Paleogene Eurasia: A review; Efforts to resolve the issue; Implications for the India-Asia collision. *Continent-Ocean Interactions within East Asian Marginal Seas, 149*, 23-35. doi:10.1029/149gm02

Ali, J. R., & Aitchison, J. C. (2008). Gondwana to Asia: Plate tectonics, paleogeography and the biological connectivity of the Indian sub-continent from the Middle Jurassic through latest Eocene (166-35 Ma). *Earth-Science Reviews, 88*(3-4), 145-166.

Alter, S. E., Brown, B., & Stiassny, M. L. J. (2015). Molecular phylogenetics reveals convergent evolution in lower Congo River spiny eels. *BMC Evolutionary Biology, 15*(1), 1-12. doi:https://doi.org/10.1186/s12862-015-0507-x

Beamish, F. W. H., Beamish, R. B., & Lim, S. L. H. (2003). Fish assemblages and habitat in a Malaysian blackwater peat swamp. *Environmental Biology of Fishes, 68*(1), 1-13. doi:Doi 10.1023/A:1026004315978

631 Beaulieu, J. M., & O'Meara, B. C. (2016). Detecting hidden diversification shifts in models of
632 trait-dependent speciation and extinction. *Systematic Biology, 65*(4), 583-601.
633 doi:10.1093/sysbio/syw022

634 Berg, L. S. (1940). Classification of fishes both Recent and fossil. *Travaux de l'Institute de*
635 *l'Academie des Sciences de l'URSS, 5*(2), 87-517 (lithoprint, J. W. Edwards, Ann Arbor,
636 1947).

637 Betancur-R, R., Broughton, R. E., Wiley, E. O., Carpenter, K., López, J. A., Li, C., . . . Ortí, G.
638 (2013). The tree of life and a new classification of bony fishes. *PLOS Currents Tree of*
639 *Life, 2013*. doi:10.1371/currents.tol.53ba26640df0ccaee75bb165c8c26288

640 Betancur-R, R., Wiley, E. O., Arratia, G., Acero, A., Bailly, N., Miya, M., . . . Ortí, G. (2017).
641 Phylogenetic classification of bony fishes. *BMC Evolutionary Biology, 17*(1), 162.
642 doi:10.1186/s12862-017-0958-3

643 Bouckaert, R., Vaughan, T. G., Barido-Sottani, J., Duchêne, S., Fourment, M., Gavryushkina, A.,
644 . . . Drummond, A. J. (2019). BEAST 2.5: An advanced software platform for Bayesian
645 evolutionary analysis. *PLOS Computational Biology, 15*(4), e1006650.
646 doi:10.1371/journal.pcbi.1006650

647 Briggs, J. C. (1989). The historic biogeography of India: isolation or contact. *Systematic*
648 *Zoology, 38*(4), 322-332. doi:Doi 10.2307/2992398

649 Briggs, J. C. (2003). The biogeographic and tectonic history of India. *Journal of Biogeography,*
650 *30*(3), 381-388.

651 Britz, R. (1994). Ontogenic features of *Luciocephalus* (Perciformes, Anabantoidei) with a
652 reversed hypothesis of anabantoid intrarelationships. *Zoological Journal of the Linnean*
653 *Society, 112*(4), 491-508.

654 Britz, R. (1996). Ontogeny of the ethmoidal region and hyopalatine arch in *Macrognathus*
655 *pancalus* (Percomorpha, Mastacembeloidei) : with critical remarks on mastacembeloid
656 inter- and intrarelationships. *American Museum Novitates, 3181*, 1-18.

657 Britz, R. (1997). Egg surface structure and larval cement glands in nandid and badid fishes, with
658 remarks on phylogeny and biogeography. *American Museum Novitates, 3195*, 1-17.

659 Britz, R., Dahanukar, N., Anoop, V. K., Philip, S., Clark, B., Raghavan, R., & Rüber, L. (2020).
660 Aenigmachannidae, a new family of snakehead fishes (Teleostei: Channoidei) from
661 subterranean waters of South India. *Scientific Reports, 10*(1), 16081. doi:10.1038/s41598-
662 020-73129-6

663 Britz, R., Kokoscha, M., & Riehl, R. (1995). The anabantoid genera *Ctenops*, *Luciocephalus*,
664 *Parasphaerichthys*, and *Sphaerichthys* (Teleostei, Perciformes) as a monophyletic group:
665 evidence from egg surface-structure and reproductive behavior. *Japanese Journal of*
666 *Ichthyology, 42*(1), 71-79.

667 Brown, K. J., Ruber, L., Bills, R., & Day, J. J. (2010). Mastacembelid eels support Lake
668 Tanganyika as an evolutionary hotspot of diversification. *BMC Evolutionary Biology, 10*,
669 188. doi:Artn 188
670 10.1186/1471-2148-10-188

671 Brownstein, C. D., Harrington, R. C., & Near, T. J. (2023). The biogeography of extant
672 lungfishes traces the breakup of Gondwana. *Journal of Biogeography, n/a*(n/a).
673 doi:https://doi.org/10.1111/jbi.14609

674 Burbrink, F. T., & Pyron, R. A. (2010). How does ecological opportunity influence rates of
675 speciation, extinction, and morphological diversification in New World ratsnakes (tribe
676 Lampropeltini)? *Evolution, 64*(4), 934-943. doi:10.1111/j.1558-5646.2009.00888.x

677 Capobianco, A., & Friedman, M. (2019). Vicariance and dispersal in southern hemisphere
678 freshwater fish clades: a palaeontological perspective. *Biological Reviews, 94*(2), 662-
679 699. doi:10.1111/brv.12473

680 Chatterjee, S., Goswami, A., & Scotese, C. R. (2013). The longest voyage: tectonic, magmatic,
681 and paleoclimatic evolution of the Indian plate during its northward flight from
682 Gondwana to Asia. *Gondwana Research, 23*(1), 238-267. doi:10.1016/j.gr.2012.07.001

683 Chatterjee, S., & Scotese, C. (2010). The wandering Indian Plate and its changing biogeography
684 during the Late Cretaceous-Early Tertiary Period. In S. Bandyopadhyay (Ed.), *New*
685 *Aspects of Mesozoic Biodiversity* (pp. 105-126). Berlin, Heidelberg: Springer Berlin
686 Heidelberg.

687 Chatterjee, S., Scotese, C. R., & Bajpai, S. (2017). Restless Indian Plate and Its epic voyage from
688 Gondwana to Asia: its tectonic, paleoclimatic, and paleobiogeographic evolution. *GSA*
689 *Special Papers, 529*, 1-147. doi:10.1130/2017.2529

690 Chen, W.-J., Bonillo, C., & Lecointre, G. (2003). Repeatability of clades as a criterion of
691 reliability: a case study for molecular phylogeny of Acanthomorpha (Teleostei) with
692 larger number of taxa. *Molecular Phylogenetics and Evolution, 26*(2), 262-288.

693 Collins, R. A., Britz, R., & Rüber, L. (2015). Phylogenetic systematics of leaffishes (Teleostei:
694 Polycentridae, Nandidae). *Journal of Zoological Systematics and Evolutionary Research,*
695 *53*(4), 259-272. doi:10.1111/jzs.12103

696 Darlington, P. J., Jr. (1957). *Zoogeography: the geographical distribution of animals*. New York:
697 John Wiley.

698 Das, B. K. (1928). III. The bionomics of certain air-breathing fishes of India, together with an
699 account of the development of their air-breathing organs. *Philosophical Transactions of*
700 *the Royal Society of London. Series B, Containing Papers of a Biological Character,*
701 *216*(431-439), 183-219. doi:10.1098/rstb.1928.0003

702 Day, J. J., Fages, A., Brown, K. J., Vreven, E. J., Stiassny, M. L. J., Bills, R., . . . Rüber, L.
703 (2017). Multiple independent colonizations into the Congo Basin during the continental

704 radiation of African *Mastacembelus* spiny eels. *Journal of Biogeography, 44*(10), 2308-
705 2318. doi:10.1111/jbi.13037

706 Dornburg, A., & Near, T. J. (2021). The emerging phylogenetic perspective on the evolution of
707 actinopterygian fishes. *Annual Review of Ecology, Evolution, and Systematics, 52*(1),
708 427-452. doi:10.1146/annurev-ecolsys-122120-122554

709 Duan, T., Shi, C., Zhou, J., Lv, X., Li, Y., & Luo, Y. (2018). How does the snakehead *Channa*
710 *argus* survive in air? The combined roles of the suprabranchial chamber and
711 physiological regulations during aerial respiration. *Biology Open, 7*(2), bio029223.
712 doi:10.1242/bio.029223

713 Dupin, J., Matzke, N. J., Sarkinen, T., Knapp, S., Olmstead, R. G., Bohs, L., & Smith, S. D.
714 (2017). Bayesian estimation of the global biogeographical history of the Solanaceae.
715 *Journal of Biogeography, 44*(4), 887-899. doi:10.1111/jbi.12898

716 Friedman, M., Feilich, K. L., Beckett, H. T., Alfaro, M. E., Faircloth, B. C., Černý, D., . . .
717 Harrington, R. C. (2019). A phylogenomic framework for pelagiarian fishes
718 (Acanthomorpha: Percomorpha) highlights mosaic radiation in the open ocean.
719 *Proceedings of the Royal Society B: Biological Sciences, 286*(1910), 20191502.
720 doi:10.1098/rspb.2019.1502

721 Friedman, M., Keck, B. P., Dornburg, A., Eytan, R. I., Martin, C. H., Hulsey, C. D., . . . Near, T.
722 J. (2013). Molecular and fossil evidence place the origin of cichlid fishes long after
723 Gondwanan rifting. *Proceedings of the Royal Society B: Biological Sciences, 280*(1770),
724 20131733. doi:doi:10.1098/rspb.2013.1733

725 Froese, R., & Pauly, D. (2022). FishBase. World Wide Web electronic publication.
726 www.fishbase.org, version (02/2022).

727 Gaudant, J. (2015). Revision of the poorly known Middle Miocene freshwater fish fauna from
728 Beuern (Hesse, Germany). *Neues Jahrbuch Fur Geologie Und Palaontologie-*
729 *Abhandlungen, 278*(3), 291-302. doi:10.1127/njgpa/2015/0529

730 Gaudant, J., & Reichenbacher, B. (1998). Première découverte d'un squelette de Channidae
731 (Poisson téléostéen) dans le Miocène inférieur d'Illerkirchberg, près d'Ulm
732 (Wurtemberg, Allemagne). *Paläontologische Zeitschrift, 72*(3), 383-388.
733 doi:10.1007/BF02988367

734 Gheerbrant, E., & Rage, J. C. (2006). Paleobiogeography of Africa: how distinct from Gondwana
735 and Laurasia? *Palaeogeography Palaeoclimatology Palaeoecology, 241*(2), 224-246.
736 doi:10.1016/j.palaeo.2006.03.016

737 Ghezelayagh, A., Harrington, R. C., Burress, E. D., Campbell, M., Buckner, J., Chakrabarty, P., .
738 . . Near, T. J. (2022). Prolonged morphological expansion of spiny-rayed fishes following
739 the end-Cretaceous. *Nature Ecology & Evolution, 6*, 1211–1220. doi:10.1038/s41559-
740 022-01801-3

741 Gosline, W. A. (1983). The relationships of the mastacembelid and synbranchid fishes. *Japanese*
742 *Journal of Ichthyology, 29*(4), 323-328. doi:10.11369/jji1950.29.323

743 Grande, L., & Bemis, W. E. (1998). A comprehensive phylogenetic study of amiid fishes
744 (Amiidae) based on comparative skeletal anatomy. An empirical search for
745 interconnected patterns of natural history. *Journal of Vertebrate Paleontology, 18*
746 *(Memoir 4)*(1), 1-690.

747 Harmon, L. J., Melville, J., Larson, A., & Losos, J. B. (2008). The role of geography and
748 ecological opportunity in the diversification of day geckos (Phelsuma). *Syst Biol, 57*(4),
749 562-573. doi:10.1080/10635150802304779

750 Harrington, R. C., Faircloth, B. C., Eytan, R. I., Smith, W. L., Near, T. J., Alfaro, M. E., &
751 Friedman, M. (2016). Phylogenomic analysis of carangimorph fishes reveals flatfish
752 asymmetry arose in a blink of the evolutionary eye. *BMC Evolutionary Biology, 16*(1),
753 224. doi:10.1186/s12862-016-0786-x

754 Hoang, D. T., Chernomor, O., von Haeseler, A., Minh, B. Q., & Vinh, L. S. (2018). UFBoot2:
755 Improving the Ultrafast Bootstrap Approximation. *Molecular Biology and Evolution,*
756 *35*(2), 518-522. doi:10.1093/molbev/msx281

757 Houle, A. (1998). Floating islands: A mode of long-distance dispersal for small and medium-
758 sized terrestrial vertebrates. *Diversity and Distributions, 4*(5-6), 201-216.

759 Hughes, G. M., & Munshi, J. S. D. (1979). Fine structure of the gills of some Indian air-
760 breathing fishes. *Journal of Morphology, 160*(2), 169-193.
761 doi:https://doi.org/10.1002/jmor.1051600205

762 Hughes, L. C., Ortí, G., Huang, Y., Sun, Y., Baldwin, C. C., Thompson, A. W., . . . Shi, Q.
763 (2018). Comprehensive phylogeny of ray-finned fishes (Actinopterygii) based on
764 transcriptomic and genomic data. *Proceedings of the National Academy of Sciences,*
765 *115*(24), 6249-6254. doi:10.1073/pnas.1719358115

766 Hui, T. H., & Ng, P. K. L. (2005a). The fighting fishes (Teleostei: Osphronemidae: Genus *Betta*)
767 of Singapore, Malaysia and Brunei. *Raffles Bulletin of Zoology, 13*, 43-99.

768 Hui, T. H., & Ng, P. K. L. (2005b). The labyrinth fishes (Teleostei: Anabantoidei, Channoidei)
769 of Sumatra, Indonesia. *The Raffles bulletin of zoology*, 115-138.

770 Ishimatsu, A., & Itazawa, Y. (1981). Ventilation of the air-breathing organ in the snakehead
771 *Channa argus*. *Japanese Journal of Ichthyology, 28*, 276-282.

772 Kosswig, C. (1955). Contributions to the historical zoogeography of African freshwater fishes.
773 *Istanbul Üniversitesi Fen Fakültesi Hidrobiologi Araştırma Enstitüsü Yayınlarından, Seri*
774 *B 2*, 83-89.

775 Kottelat, M., & Lim, K. K. P. (1994). Diagnoses of two new genera and three new species of
776 earthworm eels from the Malay peninsula and Borneo (Teleostei: Chaudhuriidae).
777 *Ichthyological Exploration of Freshwaters, 5*, 181-190.

778 Kowasupat, C., Panijpan, B., Ruenwongsa, P., & Sriwattanarothai, N. (2012). *Betta*
779 *mahachaiensis*, a new species of bubble-nesting fighting fish (Teleostei: Osphronemidae)
780 from Samut Sakhon Province, Thailand. *Zootaxa, 3522*, 49-60.

781 Lande, R., Seehausen, O., & van Alphen, J. J. M. (2001). Mechanisms of rapid sympatric
782 speciation by sex reversal and sexual selection in cichlid fish. *Genetica, 112*, 435-443.
783 doi:Doi 10.1023/A:1013379521338

784 Landis, M. J., Matzke, N. J., Moore, B. R., & Huelsenbeck, J. P. (2013). Bayesian analysis of
785 biogeography when the number of areas is large. *Systematic Biology, 62*, 789-804.
786 doi:10.1093/sysbio/syt040

787 Lanfear, R., Calcott, B., Kainer, D., Mayer, C., & Stamatakis, A. (2014). Selecting optimal
788 partitioning schemes for phylogenomic datasets. *BMC Evolutionary Biology, 14*(1), 82.
789 doi:10.1186/1471-2148-14-82

790 Lanfear, R., Frandsen, P. B., Wright, A. M., Senfeld, T., & Calcott, B. (2017). PartitionFinder 2:
791 New methods for selecting partitioned models of evolution for molecular and
792 morphological phylogenetic analyses. *Molecular Biology and Evolution, 34*(3), 772-773.
793 doi:10.1093/molbev/msw260

794 Lauder, G. V., & Liem, K. F. (1981). Prey capture by Luciocephalus pulcher: implications for
795 models of jaw protrusion in teleost fishes. *Environmental Biology of Fishes, 6*(3-4), 257-
796 268. doi:Doi 10.1007/Bf00005755

797 Lauder, G. V., & Liem, K. F. (1983). The evolution and interrelationships of the actinopterygian
798 fishes. *Bulletin of the Museum of Comparative Zoology, 150*(3), 95-197.

799 Lavoué, S. (2020). Origins of Afrotropical freshwater fishes. *Zoological Journal of the Linnean*
800 *Society, 188*(2), 345-411. doi:10.1093/zoolinnean/zlz039

801 Li, B., Dettai, A., Cruaud, C., Couloux, A., Desoutter-Meniger, M., & Lecointre, G. (2009).
802 RNF213, a new nuclear marker for acanthomorph phylogeny. *Molecular Phylogenetics*
803 *and Evolution, 50*(2), 345-363.

804 Li, X., Musikasinthorn, P., & Kumazawa, Y. (2006). Molecular phylogenetic analyses of
805 snakeheads (Perciformes: Channidae) using mitochondrial DNA sequences.
806 *Ichthyological Research, 53*(2), 148-159.

807 Liem, K. F. (1963). The comparative osteology and phylogeny of the Anabantoidei (Teleostei,
808 Pisces). *Illinois Biological Monographs, 30*, 1-149.

809 Liem, K. F. (1965). The status of the anabantoid fish genera *Ctenops* and *Trichopsis*. *Copeia,*
810 *1965*(2), 206-213. doi:10.2307/1440725

811 Liem, K. F. (1967). A morphological study of *Luciocephalus pulcher* with notes on gular
812 elements in other recent teleosts. *Journal of Morphology, 121*(2), 103-133. doi:DOI
813 10.1002/jmor.1051210203

814 Matschiner, M., Bohne, A., Ronco, F., & Salzburger, W. (2020). The genomic timeline of cichlid
815 fish diversification across continents. *Nature Communications, 11*(1). doi:ARTN 5895
816 10.1038/s41467-020-17827-9

817 Matthews, K. J., Maloney, K. T., Zahirovic, S., Williams, S. E., Seton, M., & Müller, R. D.
818 (2016). Global plate boundary evolution and kinematics since the late Paleozoic. *Global*
819 *and Planetary Change, 146*, 226-250.
820 doi:https://doi.org/10.1016/j.gloplacha.2016.10.002

821 Matzke, N. J. (2018). BioGeoBEARS: BioGeography with Bayesian (and likelihood)
822 Evolutionary Analysis with R Scripts, version 1.1.1. Published on GitHub on 6
823 November 2018.

824 McAllister, D. E. (1968). Evolution of branchiostegals and classifcation of teleostome fishes.
825 *National Museum of Canada, Bulletin, 221*, 1-239.

826 Meng, J., Wang, C., Zhao, X., Coe, R., Li, Y., & Finn, D. (2012). India-Asia collision was at
827 24°N and 50 Ma: palaeomagnetic proof from southernmost Asia. *Scientific Reports, 2*(1),
828 925. doi:10.1038/srep00925

829 Moore, B. R., Höhna, S., May, M. R., Rannala, B., & Huelsenbeck, J. P. (2016). Critically
830 evaluating the theory and performance of Bayesian analysis of macroevolutionary
831 mixtures. *Proceedings of the National Academy of Sciences, 113*(34), 9569-9574.

832 Murray, A. M. (2012). Relationships and Biogeography of the Fossil and Living African
833 Snakehead Fishes (Percomorpha, Channidae, Parachanna). *Journal of Vertebrate*
834 *Paleontology, 32*(4), 820-835. doi:Doi 10.1080/02724634.2012.664595

835 Murray, A. M., & Thewissen, J. G. M. (2008). Eocene actinopterygian fishes from Pakistan, with
836 the description of a new genus and species of channid (Channiformes). *Journal of*
837 *Vertebrate Paleontology, 28*(1), 41-52.

838 Near, T. J., Dornburg, A., Eytan, R. I., Keck, B. P., Smith, W. L., Kuhn, K. L., . . . Wainwright,
839 P. C. (2013). Phylogeny and tempo of diversification in the superradiation of spiny-rayed
840 fishes. *Proceedings of the National Academy of Sciences of the United States of America,*
841 *110*, 12738-12743. doi:10.1073/pnas.1304661110

842 Nelson, J. S. (2006). *Fishes of the world, 4th edition*. Hoboken: John Wiley.

843 Nelson, J. S., Grande, T. C., & Wilson, M. V. H. (2016). *Fishes of the world, 5th edition* (5th
844 ed.). Hoboken: John Wiley & Sons, Inc.

845 Olden, J. D., Kennard, M. J., Leprieur, F., Tedesco, P. A., Winemiller, K. O., & García-Berthou,
846 E. (2010). Conservation biogeography of freshwater fishes: recent progress and future

challenges. *Diversity and Distributions, 16*(3), 496-513. doi:https://doi.org/10.1111/j.1472-4642.2010.00655.x

Plummer, M., Best, N., Cowles, K., & Vines, K. (2006). CODA: convergence diagnosis and output analysis for MCMC. *R News, 6*, 7-11.

Rabosky, D. L. (2014). Automatic detection of key innovations, rate shifts, and diversity-dependence on phylogenetic trees. *PLOS One, 9*, e89543. doi:10.1371/journal.pone.0089543

Rabosky, D. L., Grundler, M., Anderson, C., Title, P., Shi, J. J., Brown, J. W., . . . Larson, J. G. (2014). BAMMtools: an R package for the analysis of evolutionary dynamics on phylogenetic trees. *Methods in Ecology and Evolution, 5*(7), 701-707. doi:10.1111/2041-210X.12199

Rabosky, D. L., Mitchell, J. S., & Chang, J. (2017). Is BAMM flawed? Theoretical and practical concerns in the analysis of multi-rate diversification models. *Systematic Biology, 66*(4), 477-498.

Rage, J. C. (2003). Relationships of the Malagasy fauna during the Late Cretaceous: Northern or Southern routes? *Acta Palaeontologica Polonica, 48*(4), 661-662.

Rambaut, A., Drummond, A. J., Xie, D., Baele, G., & Suchard, M. A. (2018). Posterior summarization in Bayesian phylogenetics using Tracer 1.7. *Systematic Biology, 67*(5), 901-904. doi:10.1093/sysbio/syy032

Rosen, D. E., & Greenwood, P. H. (1976). A fourth Neotropical species of synbranchid eel and the phylogeny and systematics of synbranchiform fishes. *Bulletin of the American Museum of Natural History, 157*, 1-69.

Rosen, D. E., & Patterson, C. (1990). On Müller's and Cuvier's concepts of pharyngognath and labyrinth fishes and the classification of percomorph fishes, with an atlas of percomorph dorsal gill arches. *American Museum Novitates, 2983*, 1-57.

Rüber, L., Britz, R., Kullander, S. O., & Zardoya, R. (2004). Evolutionary and biogeographic patterns of the Badidae (Teleostei: Perciformes) inferred from mitochondrial and nuclear DNA sequence data. *Molecular Phylogenetics and Evolution, 32*(3), 1010-1022.

Rüber, L., Britz, R., Tan, H. H., Ng, P. K. L., & Zardoya, R. (2004). Evolution of mouthbrooding and life-history correlates in the fighting fish genus *Betta*. *Evolution, 58*(4), 799-813.

Rüber, L., Britz, R., & Zardoya, R. (2006). Molecular phylogenetics and evolutionary diversification of labyrinth fishes (Perciformes: Anabantoidei). *Systematic Biology, 55*(3), 374-397.

Rüber, L., Tan, H. H., & Britz, R. (2020). Snakehead (Teleostei: Channidae) diversity and the Eastern Himalaya biodiversity hotspot. *Journal of Zoological Systematics and Evolutionary Research, 58*(1), 356-386. doi:https://doi.org/10.1111/jzs.12324

Sanciangco, M. D., Carpenter, K. E., & Betancur-R, R. (2016). Phylogenetic placement of enigmatic percomorph families (Teleostei: Percomorphaceae). *Molecular Phylogenetics and Evolution, 94, Part B*, 565-576. doi:http://dx.doi.org/10.1016/j.ympev.2015.10.006

Schindler, I., & Schmidt, J. (2009). Betta kuehnei, a new species of fighting fish (Teleostei, Osphronemidae) from the Malay Peninsula. *Bulletin of Fish Biology, 10*, 1-8.

Seehausen, O. (2000). Explosive speciation rates and unusual species richness in haplochromine cichlid fishes: Effects of sexual selection. *Advances in Ecological Research, Vol 31, 31*, 237-274.

Sholihah, A., Delrieu-Trottin, E., Condamine, F. L., Wowor, D., Ruber, L., Pouyaud, L., . . . Hubert, N. (2021). Impact of Pleistocene eustatic fluctuations on evolutionary dynamics in southeast asian biodiversity hotspots. *Systematic Biology, 70*(5), 940-960. doi:10.1093/sysbio/syab006

Sholihah, A., Delrieu-Trottin, E., Sukmono, T., Dahruddin, H., Pouzadoux, J., Tilak, M.-K., . . . Hubert, N. (2021). Limited dispersal and in situ diversification drive the evolutionary history of Rasborinae fishes in Sundaland. *Journal of Biogeography, n/a*(n/a). doi:https://doi.org/10.1111/jbi.14141

Simpson, G. G. (1953). *The major features of evolution*. New York,: Columbia University Press.

Springer, V. G., & Johnson, G. D. (2004). Study of the dorsal gill-arch musculature of teleostome fishes, with special reference to the Actinopterygii. *Bulletin of the Biological Society of Washington, 11*, 1-260.

Steinitz, H. (1954). The distribution of the fresh-water fishes of Palestine. *Istanbul Üniversitesi Fen Fakültesi Hidrobiologi Araştırma Enstitüsü Yayınlarından, Seri B 1*, 225-275.

Stroud, J. T., & Losos, J. B. (2016). Ecological Opportunity and Adaptive Radiation. *Annual Review of Ecology, Evolution, and Systematics, 47*, 507-532.

Tate, M., McGoran, R. E., White, C. R., & Portugal, S. J. (2017). Life in a bubble: the role of the labyrinth organ in determining territory, mating and aggressive behaviours in anabantoids. *Journal of Fish Biology, 91*(3), 723-749. doi:https://doi.org/10.1111/jfb.13357

Tran, L. A. (2014). The role of ecological opportunity in shaping disparate diversification trajectories in a bicontinental primate radiation. *Proc Biol Sci, 281*(1781), 20131979. doi:10.1098/rspb.2013.1979

Wainwright, P. C., Smith, W. L., Price, S. A., Tang, K. L., Sparks, J. S., Ferry, L. A., . . . Near, T. J. (2012). The evolution of pharyngognathy: a phylogenetic and functional appraisal of the pharyngeal jaw key innovation in labroid fishes and beyond. *Systematic Biology, 61*(6), 1001-1027. doi:10.1093/sysbio/sys060

Wu, F., He, D., Fang, G., & Deng, T. (2019). Into Africa via docked India: a fossil climbing perch from the Oligocene of Tibet helps solve the anabantid biogeographical puzzle. *Science Bulletin, 64*(7), 455-463. doi:https://doi.org/10.1016/j.scib.2019.03.029

Zhang, C., Rabiee, M., Sayyari, E., & Mirarab, S. (2018). ASTRAL-III: polynomial time species tree reconstruction from partially resolved gene trees. *BMC Bioinformatics, 19*(6), 153. doi:10.1186/s12859-018-2129-y